

Conductance Anomalies for Normal-Insulator-Superconductor Contacts

Sungkit Yip

*Department of Physics & Astronomy, Northwestern University, Evanston, IL 60208 **

(May 25, 2018)

This paper considers the conductance through a dirty junction between a normal conductor and a superconductor with an insulating barrier. It is shown that for large barrier resistances there is a relative enhancement of the conductance near zero voltage, whereas for low barrier resistance this anomaly appears at finite voltage.

PACS numbers: 74.80.Fp, 74.50.+r

Recent experiments on contacts between semiconductors and superconductors have generated a lot of interest (see e.g. [1–5] and references therein). Besides possible technical application of these devices, one is interested in understanding how electrical conductance below the superconducting gap arises. While there is little doubt that the basic process is Andreev reflection [6], the role of impurities is only being appreciated gradually recently. The interplay between impurity scattering and the potential scattering at the Schottky barrier between the semiconductor and superconductor is believed [7–14] to be the physics behind the zero bias anomaly (ZBA) observed in many experiments (e.g. [1–5])

To understand the transport in these normal-insulator-superconductor structures two major theoretical tools have been employed. In Ref [13,14] the conductance is expressed in terms of the transmission matrices across the structure. Unfortunately quite often the necessary averages are not available from random matrix theory and thus numerical calculations to obtain the transmission matrices have to be done for a large number of "samples" and then averages over the samples taken. An alternative approach [7–10] is to use the quasiclassical green's function where the impurity average has already been made. However, in this approach the impurity scattering is only included in the self-consistent Born approximation. Moreover these references confined themselves to the cases of high potential barriers (and often low energies) so that analytical progress can be made, although the basic equations are applicable more generally so long as we are in the dirty limit. In this paper we shall solve these equations numerically in order to obtain a better understanding of the physics as well as a detail comparison with the results from the scattering matrix approaches. [13,14]

We shall then consider a (quasi-one-dimensional) normal conductor ("wire") situated between a normal ($x = 0$) and a superconducting ($x = L$) reservoirs. The reservoirs are assumed to be at equilibrium at potential V and 0 respectively. A potential barrier is located at x_b where $0 \leq x_b \leq L$. We shall confine ourselves to the dirty limit where all the energy scales are smaller than the impurity scattering rate. We also require that the mean free path l to be much less than L . (Note that experiments cited above may not satisfy this condition). We shall assume that there is no pairing interaction in our conducting "wire" and we shall consider only ordinary and magnetic impurity scatterings. To study the transport through the system we shall solve the Usadel equation

$$[\epsilon\tau_3 - \check{\sigma}_{spin}, \check{g}] + \frac{D}{\pi}\partial_\mu(\check{g}\partial_\mu\check{g}) = 0 \quad (1)$$

together with the normalization condition $\check{g}^2 = -\pi^2\check{1}$ governing the angular averaged Green's function

$$\check{g} = \begin{pmatrix} \hat{g}^R & \hat{g}^K \\ 0 & \hat{g}^A \end{pmatrix}$$

and $\hat{g}^{R,A,K}$ are the retarded, advanced, and Keldysh matrix Green's functions in particle-hole and spin space. Here ϵ is the energy and $\hat{\sigma}_{spin}^{R,A,K} = \frac{\gamma}{2\pi}\hat{\tau}_3\hat{g}^{R,A,K}\hat{\tau}_3$ is the self-energy for magnetic scattering with the scattering rate γ . The equation connecting \check{g} on the two sides of an interface has been derived by Kuprianov and Lukichev [15],

$$\bar{\sigma}S\check{g}\partial_\mu\check{g} = \frac{G_b^n}{2}[\check{g}(x_{b-}), \check{g}(x_{b+})] \quad (2)$$

$\bar{\sigma}$ is the conductivity of the wire, S the area, and G_b^n is the conductance through of the barrier in the **normal** state. For our purpose \hat{g}^R can be chosen to have only τ_3 and $\sigma_2\tau_1$ components: $\hat{g}^R = -i\pi(g_3\tau_3 - f_1\sigma_2\tau_1)$. \hat{g}^A is related to

*electronic mail: yip@sneffels.phys.nwu.edu

\hat{g}^R by $\hat{g}^A = \tau_3(\hat{g}^R)^\dagger\tau_3$. Since $g_3^2 + f_1^2 = 1$ from the normalization condition, we can write $g_3 = \cos\theta$ and $f_1 = \sin\theta$ where $\theta \equiv \theta_r + \theta_i$ is in general complex. From eq(1) θ satisfies

$$2i(\epsilon + i\gamma\cos\theta)\sin\theta + D\partial_x^2\theta = 0 \quad (3)$$

The boundary condition eq(2) reduces to

$$(\bar{\sigma}S)\partial_x\theta = G_b^n \sin([\theta]_b) \quad (4)$$

here $[\theta]_b$ is the discontinuity of θ across the interface, i.e., $[\theta]_b = \theta(x_{b+}) - \theta(x_{b-})$. θ at $x = 0$ and $x = L$ are assumed to attain their equilibrium values of the reservoirs. Thus at $x = 0$ $\theta_r = \theta_i = 0$ and at $x = L$, $\theta_r = \frac{\pi}{2}$, $\theta_i = \frac{1}{2}\ln\frac{\Delta+\epsilon}{\Delta-\epsilon}$, i.e., $\tanh\theta_i = \frac{\epsilon}{\Delta}$ for $\epsilon < \Delta$. (and $\theta_r = 0$, $\theta_i = \frac{1}{2}\ln\frac{\epsilon+\Delta}{\epsilon-\Delta}$, for $\epsilon > \Delta$).

We can define a distribution function \hat{h} by $\hat{g}^K = \hat{g}^R\hat{h} - \hat{h}\hat{g}^A$ where \hat{h} can be chosen diagonal $\hat{h} = h_0\hat{\tau}_0 + h_3\hat{\tau}_3$. For our purposes it is sufficient to solve for h_3 , which satisfies (from eq(1))

$$\partial_x(\cosh^2\theta_i\partial_x h_3) = 0 \quad (5)$$

in the bulk together with the boundary condition (from eq(2))

$$(\bar{\sigma}S)\cosh^2\theta_i\partial_x h_3 = G_b^n \cos([\theta_r]_b)\cosh\theta_i(x_{b+})\cosh\theta_i(x_{b-})[h_3]_b \quad (6)$$

Here $[h_3]_b$ is the discontinuity of h_3 across the barrier. For a potential V applied to the normal reservoir at $x = 0$ and zero potential at the superconducting reservoir, we have then $h_3(\epsilon) = \frac{n(\epsilon+eV)-n(\epsilon-eV)}{2}$ at $x = 0$ and $h_3(\epsilon) = 0$ at $x = L$. Here $n(\epsilon) = \tanh\frac{\epsilon}{2T}$. We shall confine ourselves to zero temperature, where $n(\epsilon)$ becomes a step function. Thus $h_3(\epsilon)$ decreases from 1 at $x = 0$ to 0 at $x = L$ if $|\epsilon| < eV$, and is identically zero otherwise. Since the current $I(V) = \frac{\bar{\sigma}S}{e} \int_{-\infty}^{\infty} \frac{d\epsilon}{16\pi^2} \text{tr}[\tau_3(\hat{g}^R\partial_x\hat{g}^K + \hat{g}^K\partial_x\hat{g}^A)]$ can be written as $I(V) = -\frac{\bar{\sigma}S}{e} \int_0^\infty d\epsilon \cosh^2\theta_i\partial_x h_3$, the conductance $G(V) \equiv \frac{dI}{dV}$ at voltage V is given by

$$G(V) = -\bar{\sigma}S \cosh^2\theta_i\partial_x h_3|_{\epsilon=eV} \quad (7)$$

It is obvious from the discussion above and eqs(5,6) that h_3 behaves like a voltage along a wire with (position dependent) conductivity $\bar{\sigma}S \cosh^2\theta_i$ in series with a resistor with conductance

$$G_T(V) = G_b^n \cos([\theta_r]_b)\cosh\theta_i(x_{b+})\cosh\theta_i(x_{b-})|_{\epsilon=eV} \quad (8)$$

and can be easily found. h_3 of course should not be taken literally as the voltage itself, but the concept of these effective conductances will help us understand our results. The conductance through the system can therefore be written as

$$G(V) = (R_1(V) + R_T(V) + R_2(V))^{-1} \quad (9)$$

where

$$R_1(V) = \frac{1}{\bar{\sigma}S} \int_0^{x_b} dx \text{sech}^2\theta_i(x)|_{\epsilon=eV} \quad (10)$$

and similarly for R_2 except the integration limits are from x_b to L and $R_T \equiv (G_T(V))^{-1}$. The above equations have essentially been derived in ref. [8,11]

Before describing our results it is helpful to discuss the physical meanings of θ_r and θ_i . The usual density of states is given by $\text{Reg}_3 = \cos\theta_r \cosh\theta_i$. Notice however this is not the quantity that is directly relevant to the effective conductances through the wire or the barrier. As seen from eqs(10) and (8) the relevant factors are $\cosh^2\theta_i = (\text{Reg}_3)^2 + (\text{Ref}_1)^2$ and $\cos([\theta_r]_b)\cosh\theta_i(x_{b+})\cosh\theta_i(x_{b-}) = (\text{Reg}_3(x_{b-}))(\text{Reg}_3(x_{b+})) + (\text{Ref}_1(x_{b-}))(\text{Ref}_1(x_{b+}))$ respectively. Notice also under a unitary transformation between the particle and hole components of opposite spin (i.e., a generalized Bogoliubov transformation), \hat{g}^R transforms into $\hat{g}'^R = e^{i\frac{\chi}{2}\sigma_2\tau_2}\hat{g}^R e^{-i\frac{\chi}{2}\sigma_2\tau_2}$ where χ is a real number. If one parametrizes \hat{g}'^R by θ' as before then $\theta'_r = \theta_r + \chi$ and $\theta'_i = \theta_i$. It is thus useful to think of θ_r as the angle of a vector in an imaginary space which I shall refer to as spectral space (see also [16]), and $\cosh\theta_i$ as its magnitude. The equation of motion for θ_r and θ_i is given by eq(3) and (4). Reg_3 and Ref_1 are then the two (g - and f -) components of the spectral vector or the density of states vector (DOSV). The effective conductance of the conductor at a given point and voltage is thus enhanced by the square of the DOSV (at that point and voltage), while the conductance through

a barrier is modified by the factor corresponding to the scalar product of the spectral vector on the two sides. Both these factors are invariants under the particle-hole transformation. Conductance through a barrier is thus possible only when the spectral vectors on the two sides have finite projection onto each other. For a direct contact between a normal metal ($\theta_r = 0$) and a superconductor ($\theta_i = 0$ for $\epsilon < \Delta$) there is thus no subgap conductance. In the NIS structure as in here the finite resistivity of the wire allows $\theta_r \neq 0$ at x_{b-} and hence a finite barrier conductance.

We shall concentrate on the subgap conductance $eV \ll \Delta$. For a better display of the θ parameters in Fig. 4 below, I have chosen to present the results for $x_b = 0.92L$. The results for the total resistances presented below are virtually independent of x_b so long as $x_b \approx L$. From the above equations it is convenient to define a dimensionless parameter g_b as the ratio of the normal state conductances through the barrier to that of the wire, i.e. $g_b = G_b^n / G_{wire}^n$, where $G_{wire}^n = \bar{\sigma}S/L$. We shall also express all energies in terms of the natural scale $E_D \equiv D/L^2$. The gap Δ is chosen to be $100E_D$.

Fig. 1 shows the conductance of our NIS system for intermediate values of g_b . For $g_b \lesssim 1.0$ we obtain the an anomaly at zero bias (ZBA). At higher g_b 's an anomaly at finite voltage (FBA) is apparent. The position of this FBA is roughly $\sim g_b E_D$ for these intermediate values. (see however below). This FBA is actually built on top of a ZBA. Fig. 2 shows the effect of magnetic scattering on the FBA for $g_b = 2.5$. We see that the FBA is sensitive to γ , and is removed for $\gamma \sim g_b E_D$ (also see, however, below). The ZBA remains after the FBA is destroyed.

To understand these features, it is helpful to consider the 'resistances' defined in eqs (8) and (10), as shown in Fig. 3 again for $g_b = 2.5$. [17] The FBA results from the dip at finite voltage for R_1 (more precisely $R_1 + R_2$, the total effective resistance for the wire), whereas the ZBA is from the minimum at zero voltage for R_T . The relatively small γ ($\sim g_b E_D$ for these intermediate g_b) first remove the feature in R_1 . The minimum at $V = 0$ for R_T is somewhat more robust.

The features for R_1 and R_T can in turn be related to the behavior of θ_r and θ_i . (recall eqs(8) and (10). It is also helpful to observe that a natural length scale $\sqrt{\frac{D}{\epsilon}}$ i.e., the coherence length at energy ϵ , arises in eq (3)) Fig. 4 shows these parameters again for $g_b = 2.5$ and for a specific energy $\epsilon = 2.5$. First consider $\gamma = 0$. We see that θ_i is finite within the wire, but small at the two ends ($\theta_i \approx 0$ at $x = L$ because $\epsilon \ll \Delta$). This θ_i is generated from the gradients, as is evident from taking the imaginary part of eq(3) : at finite ϵ and θ_r there is a contribution to a negative curvature of θ_i in the form of $\frac{2\epsilon}{D} \sin\theta_r \cosh\theta_i$. Fig. 5 shows the values of θ_r and θ_i at the immediate left of the barrier (x_{b-}) for two values of g_b at $\gamma = 0$. These values are good indicators of the values of θ_r and θ_i within the wire if we keep in mind their typical spatial dependence as in Fig. 4. As the energy increases $\theta_i(x_{b-})$ first increases, then saturates and shows a slight decrease afterwards. This gives rise to the shape of R_1 . At larger energies θ_r decreases faster from the boundary towards $x = 0$, thus acquiring a larger slope at the boundary and hence a larger $[\theta_r]_b$ (as well as a smaller value within the wire which slow the increase of θ_i as just mentioned), and gives rise to the increase of R_T as a function of voltage. For smaller g_b 's the resistance is dominated by R_T , where the angle between the spectral vectors on the two sides of the barrier are also larger. Thus for smaller g_b as a function of voltage R_T increases rapidly with voltage and dominates the resistance, and only the ZBA but not the FBA remains. Thus in short the ZBA is due to the tilting of the spectral vector at x_{b-} at low voltages away from $\theta_r = 0$ due to the proximity effect, and the FBA is due to the fact that at finite energies a spatial gradient increases the magnitude of the DOSV within the wire. The presence of a small γ suppresses the negative curvature of θ_i and thus θ_i itself, thus destroying the FBA. γ also increases the curvature of θ_r and thus $[\theta_r]_b$, which contributes to the suppression of the ZBA. (see Fig. 4)

An example for the conductance at small g_b (0.1) is shown in Fig. 6. [19] It is interesting to note that the curves for different γ 's actually cross each other at $eV \gtrsim E_D$, i.e., for some "large" voltage that G actually increases with increasing pair-breaking. This anomalous dependence has also been found by Volkov and Klapwijk [9] for the double barrier structures for large barrier resistances. It is not clear how to understand this physically.

For very large g_b the resistance of the system comes almost entirely from the wire, and the FBA is most prominent. The position of the FBA as well as the γ needed to destroy the FBA seems to saturate for large γ (at $\sim 5E_D$ and $\sim 3E_D$ respectively): see Fig. 7 ($g_b = 24$). Since increasing ϵ tends to increase θ_i , for large γ the conductance actually has a minimum at $eV = 0$ and increases with increasing voltage.

It is of interest to compare Figs 1,2,6,7 with the results of Marmorkos et al [14], who have studied the ZBA and FBA by employing the scattering matrix method. The qualitative behaviors of the conductance are similar. Our FBA seems to be located at a similar value of eV and has similar width [18]. However, important differences have to be noted. It is useful first to recall that the normal state conductance of the system is $G_{wire}^n / (1 + g_b^{-1})$ (e.g. $0.8G_{wire}^n$ for $g_b = 4.0$ and $0.96G_{wire}^n$ for $g_b = 24$). Hence for $g_b \gtrsim 4$ the conductances at $eV = 0$ are almost the normal state values, and for the voltages shown for these g_b 's the conductances are always larger than the corresponding normal state values except for very small voltages. The conductances at $eV = 0$ found in [14] are smaller than the normal state even for perfectly transmitting interface, and only overshoot the normal state value near the FBA for relatively

transparent barriers [20].

Marmorkos et al [14], and Takane and Ebisawa (TE) [13] had also examined the effect of magnetic field B on the conductance at zero voltage. The magnetic field makes the problem intrinsically (at least) two dimensional in general and we hope to return to that in the future. However, since the magnetic field is also a pair-breaker it is of interest to compare their results with Fig. 2, 6 and 7. It is obvious from our plots that $G(V = 0, \gamma)$ always decreases with increasing γ . The relative change in G (i.e. the change measured in $G(V = 0, \gamma)/G(V = 0, \gamma = 0)$) decreases as the barrier resistance decreases, and vanishes as $g_b \rightarrow \infty$ (see Fig. 7, and also [17]). In TE [13] the behavior of $G(V = 0, B)$ as a function of increasing magnetic field B is similar to the one for $G(V = 0, \gamma)$ just described. However in Marmorkos et al although $G(V = 0, B)$ still decreases with B for high potential barriers, it increases with field for the transparent interface. It is unclear why the results of Marmorkos et al and TE are different.

For normal metals if $v_f \sim 10^8 \text{ cm/sec}$ and $L \sim \mu\text{m}$, then $E_D \sim 0.02 \text{ meV}$ if $l \sim 1000 \text{ \AA}$. To observe the FBA the condition $G_b^n > G_{wire}^n$ roughly requires the transmission probability (appropriately angular averaged) through the barrier to be $\gtrsim 0.1$, which should be easily achievable for a suitable choice of the metal and the superconductor. To observe the FBA in the semiconductor-superconductor system seems to be not so easy. Even for a choice of semiconductor like InGaAs where the tunneling through the Schottky barrier is enhanced by the small effective mass, since the Fermi wavelength on the two sides differ significantly most of the excitations are still reflected. In order to get $G_b^n > G_{wire}^n$ smaller l and/or larger L have to be chosen, making E_D much smaller. One should also keep in mind that most of the recent experiments on these structures involve semiconductors in the clean limit, where the present calculation does not apply.

This research is supported by the National Science Foundation through the Northwestern University Materials Science Center, grant number DMR 91-20521.

- [1] T. M. Klapwijk, *Physica B* **197**, 481 (1994)
- [2] A. Kastalsky et al, *Phys. Rev. Lett.* **67**, 3026 (1991).
- [3] C. Nguyen et al, *Phys. Rev. Lett.* **69**, 2847 (1992).
- [4] J. Nitta et al, *Phys. Rev.* **B 49**, 3659 (1994).
- [5] S. J. M. Bakker et al, *Phys. Rev.* **B 49**, 13275 (1994)
- [6] A. F. Andreev, *JETP*, **19**, 1228 (1964)
- [7] A. V. Zaitsev, *JETP Lett.*, **51**, 41 (1990)
- [8] A. F. Volkov, *JETP Lett.*, **55**, 747 (1992)
- [9] A. F. Volkov and T. M. Klapwijk, *Phys. Lett. A* **168**, 217 (1992)
- [10] A. F. Volkov, A. V. Zaitsev and T. M. Klapwijk, *Physica (Amsterdam)* **210C**, 21 (1993)
- [11] A. F. Volkov, *Physica* **B 203**, 267 (1994)
- [12] B. J. van Wees et al, *Phys. Rev. Lett.* **69**, 510 (1992)
- [13] Y. Takane and H. Ebisawa, *J. Phys. Soc. Jpn* **62**, 1844 (1993).
- [14] I. K. Marmorkos, C. W. J. Beenakker and R. A. Jalabert, *Phys. Rev.* **B 48**, 2811 (1993)
- [15] M. Yu. Kuprianov and V. F. Lukichev, *JETP* **67** 1163 (1988)
- [16] Yu. V. Nazarov *Phys. Rev. Lett.* **73**, 134 (1994)
- [17] Notice that $R_1(V = 0)$ is simply $0.92R_{wire}^n$ (recall $x_b = 0.92L$) and is independent of γ since we always have $\theta_i(x) = 0$ at $\epsilon = 0$ (see eq(3). However, typically $R_T > R_b^n (= g_b^{-1}R_{wire}^n = 0.4R_{wire}^n$ here), which is due to the $\cos[\theta_r]_b$ factor.
- [18] See their Fig. 2a. Note that since their calculation is for a two dimensional lattice their $E_c \equiv \frac{\pi}{2} \frac{v_f l}{L}$ should correspond to $\sim 3.14E_D$ here).
- [19] Notice that for $\gamma = 0$ the width of the ZBA here is still $\sim E_D$, not $\sim g_b^2(1 + g_b)^2/4$ as the calculation of ref [9] for double barrier systems would seem to suggest if we put one of their barrier resistance to zero.
- [20] As $g_b \rightarrow \infty$ there is no barrier. Our result here is in accordance with that of Artemenko et al *Sol. State. Comm.* **30** 771 (1979) (See also Y. Takane and H. Ebisawa, *J. Phys. Soc. Jpn* **61**, 2858 (1992); C. W. J. Beenakker *Phys. Rev.* **B 46**, 12841 (1992), and ref [16]) that the resistance of the wire connecting N and S for $V \rightarrow 0$ is the same as that in the normal state in the limit $L \gg l$. Thus this difference may be due to a finite l/L correction.

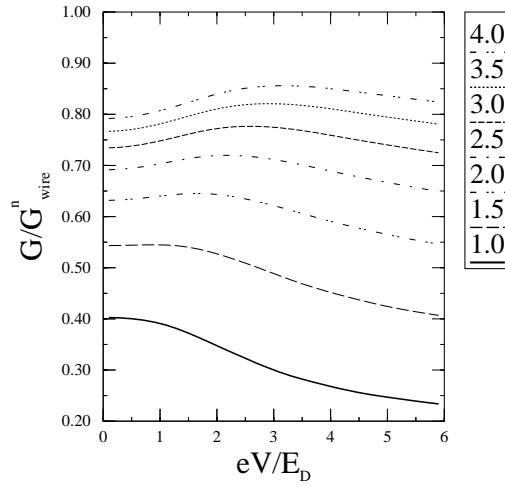


FIG. 1. The (normalized) conductance versus voltage for g_b 's listed in the legend. $\gamma = 0$.

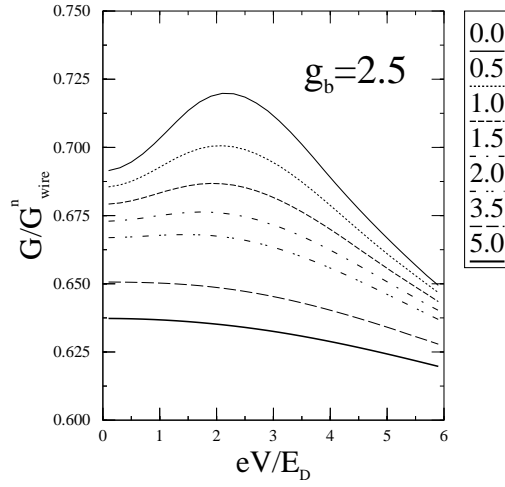


FIG. 2. The (normalized) conductance versus voltage at $g_b = 2.5$ for the values of γ listed in the legend.

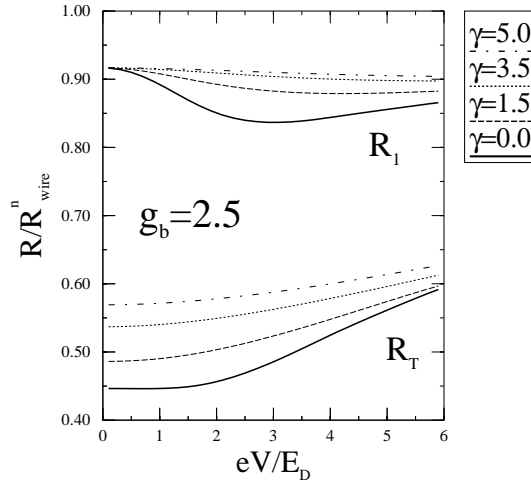


FIG. 3. The effective "resistances" R_I and R_T for $g_b = 2.5$ for some values of γ listed in the legend. $R_{wire}^n \equiv (G_{wire}^n)^{-1}$. R_2 is very small, roughly constant ($\sim 0.08R_{wire}^n$) and is not shown here.

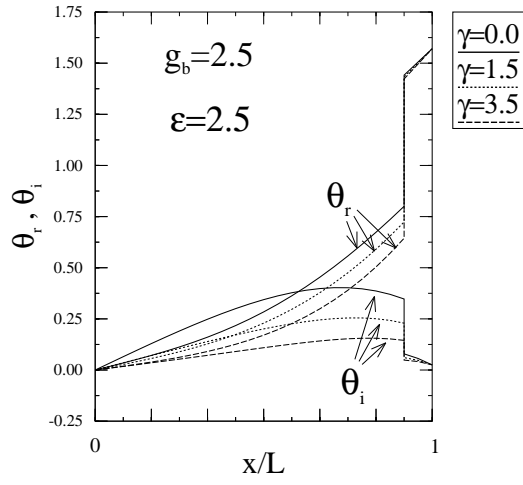


FIG. 4. The parameters θ_r and θ_i for $g_b = 2.5$ and $\epsilon = 2.5$ for some values of γ listed in the legend.

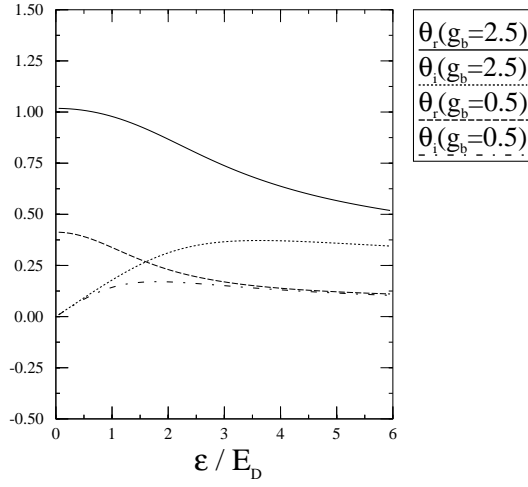


FIG. 5. The parameters θ_r and θ_i at x_{b-} for $g_b = 2.5$ and $g_b = 0.5$ as a function of energy. $\gamma = 0$.

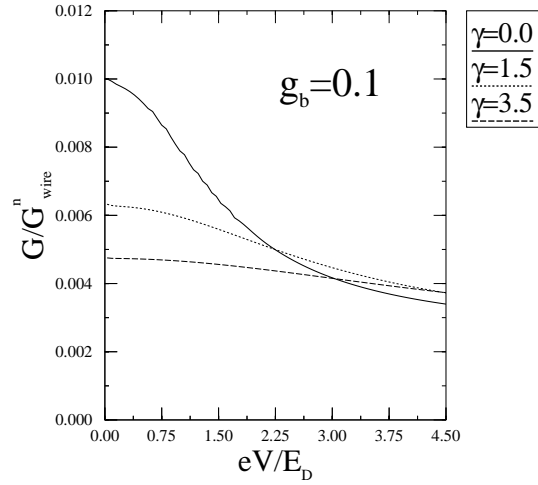


FIG. 6. The (normalized) conductance versus voltage at $g_b = 0.1$ for the values of γ listed in the legend.

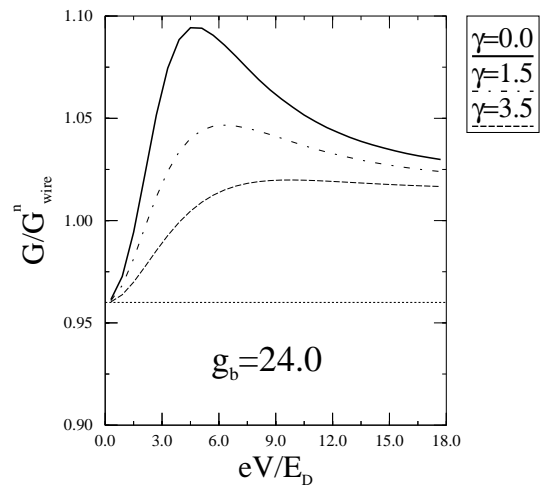


FIG. 7. The (normalized) conductance versus voltage at $g_b = 24$ for the values of γ listed in the legend. The horizontal dotted line is the normal state conductance of the system.